

# AN IMPLICIT ATTENTION MECHANISM FOR DEEP LEARNING PEDESTRIAN RE-IDENTIFICATION FRAMEWORKS

Ehsan Yaghoubi<sup>\*†</sup> Diana Borza<sup>§</sup> Aruna Kumar<sup>\*</sup> Hugo Proena<sup>\*†</sup>

<sup>\*</sup>IT: Instituto de Telecomunicações, <sup>†</sup>University of Beira Interior, Portugal

<sup>§</sup>Technical University of Cluj-Napoca, Romania

## ABSTRACT

*Attention*<sup>1</sup> is defined as the preparedness for the mental selection of certain aspects in a physical environment. In the computer vision domain, this mechanism is of most interest, as it helps to define the segments of an image/video that are critical for obtaining a specific decision. This paper introduces one *implicit* attentional mechanism for deep learning frameworks, that provides simultaneously: 1) masks-free; and 2) foreground-focused samples for the inference phase. The main idea is to generate synthetic data composed of interleaved segments from the original learning set, while using class information only from specific segments. During the learning phase, the newly generated samples feed the network, keeping their label exclusively consistent with the identity from where the region-of-interest was cropped. Hence, as the model receives images of each identity with inconsistent unwanted areas, it naturally pays the most attention to the label consistent consistent regions, which we observed to be equivalent to learn an effective receptive field. During the test phase, samples are provided without any mask, and the network naturally disregards the detrimental information, which is the insight for the observed improvements in performance. As a proof-of-concept, we consider the challenging problem of pedestrian re-identification and compare the effectiveness of our solution to the state-of-the-art techniques in the well known *Richly Annotated Pedestrian* (RAP) dataset. The code is available at <https://github.com/Ehsan-Yaghoubi/reid-strong-baseline>.

**Index Terms**— Person Re-identification, Attention Networks, Data Augmentation, Deep Learning.

## 1 Introduction

Person Re-identification (Re-ID) refers to the cross-camera retrieval task, in which a query from a target subject

This research is funded by the FEDER, Fundo de Coesao e Fundo Social Europeu under the PT2020 - Portugal 2020 program, IT: Instituto de Telecomunicações and TOMI: Citys Best Friend. Also, the work is funded by FCT/MEC through national funds and, when applicable, co-funded by the FEDER PT2020 partnership agreement under the project UID/EEA/50008/2019.

<sup>1</sup><https://www.nature.com/articles/nrn1903>

is used to retrieve visually similar images and identities from a gallery set. This process raises several difficulties, such as variations in human poses, camera resolution, and cluttered backgrounds. The primary way to address these challenges is to provide large-scale training data, which are not only hard to collect but can be particularly costly to annotate—in case of using supervised classification frameworks.

Recently, various approaches have been proposed for image synthesizing and data augmentation [1]. For example, [2] generates  $N^2$  samples from an  $N$ -sized dataset by using a sample pairing method, in which a random couple of images are overlaid based on the average intensity values of their pixels. [3] presents a *random erasing* data augmentation strategy that inflates the training data by randomly selecting rectangular regions and changing their pixels values. Increasing the volume of the training data, as an attempt to robust the model against occlusions, turned the concept of *random erasing* into a popular data augmentation technique.

When compared particularly to [2] and [3], the work described in this paper can be seen as a data augmentation technique with several singularities: 1) we not only enlarge the training data but also implicitly provide the inference model with an attentional decision-making skill; the insight is based on the foreground-background swapping that provides an ROI-focused model, contributing to ignore the background and irrelevant features during the test phase. 2) we generate highly representative samples, making it possible to use our solution along with other data augmentation methods; and 3) our solution allows the on-the-fly data generation, which is essential for computational purposes. The results of our experimental evaluation on the RAP dataset for different probabilities and loss functions confirm the consistent superiority of our strategy over the state-of-the-art approaches.

## 2 Related Work

**Attention Mechanism.** *Where to look at in an image?* is a challenging question for mimicking the human attention mechanism. Some approaches prioritize the processing of the critical regions based on local, low-level features or landmarks [4], while others gather the information sequentially and decide what regions to exploit upon the previous steps

[5]. In opposition to previous works that implement the attentional process explicitly in the deep-based frameworks [5], we provide an attentional control ability based on augmentative data preprocessing, as detailed in section 3.

**Data Augmentation.** Data augmentation targets the root cause of the overfitting problem (i.e., the training set) by generating new data samples and preserving their ground truth labels. *Geometrical transformation* (scaling, rotations, flipping, etc.), *color alteration* (contrast, brightness, hue), *image manipulation* (random erasing [3], kernel filters, image mixing [2]), and *deep learning approaches* (neural style transfer, generative adversarial networks) [1] are the common augmentation techniques.

**Person Re-ID.** In general, person Re-ID methods study either the descriptors to extract more robust feature representations or metric-based methods to handle the distance between the inter-class and intra-class samples. From the deep learning point of view, Re-ID approaches can be divided into three branches: i) *Convolutional Neural Network (CNN)*. A series of studies introduce novel network structures by relying on the body-part models and extracting the local features [6], while some works propose structures that simultaneously receive two or more images [7] and extract better discriminative features. Some other authors have suggested multi-model structures [8] to learn more patterns from multiple datasets or multiple domains [9]. ii) *CNN-Recurrent neural network*. Some prior researchers improved the performance of the person Re-ID approaches using multi-frame structures [10]. Among these methods, [11] suggests learning the key features of several frames to decrease the complexity of the network. iii) *Generative Adversarial Network (GAN)*. [12], [13] are some studies that employ GAN to generate new data and increase the generalization ability of the model for solving pedestrian Re-ID problems.

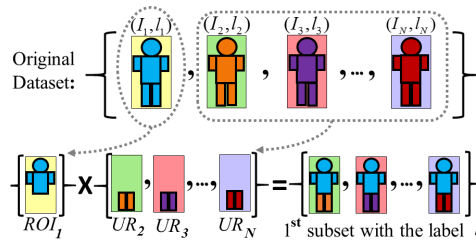
### 3 Proposed Method

Figure 1 provides an overview of the proposed image synthesis method, in this case considering the upper-body as the region of interest (ROI). We show the generated synthetic set, in which the samples are composed of the upper-body (ROI) of the 1<sup>st</sup> sample, and remaining segments from other samples, while keeping the label of the 1<sup>st</sup> sample.

#### 3.1 Attentional Data Augmentation

As an intrinsic behavior of CNNs, in the training phase, the network extracts a set of meaningful features in accordance with the image annotations. However, extracting relevant and compressed features is an ongoing challenge, especially when different identities appear with various backgrounds<sup>2</sup> and body-poses. Intuitively, when pose and back-

<sup>2</sup>Phrases (*unwanted region/region of interest*), (*undesired/desired*) *boundaries*, (*background/foreground*) *areas*, and (*unwanted/wanted*) *areas* refer to the portion of an image that is (irrelevant/relevant) to the ground truth labels.



**Fig. 1:** Upper-body attentional data augmentation provides synthesized samples with the upper-body annotations and causes an early discovery: background features are meaningless for person re-identification. Blue, orange, purple, and red indicate the sample 1, 2, 3, and  $N$ , respectively, and pale-yellow, -green, -pink, and -purple colors show their non-person regions. Therefore, fake images of a sample 1 have the same blue upper-body and ID label with different backgrounds (i.e., lower-bodies and non-person regions.)

ground are changed alongside the person identity, some misleading features of the background and pose are entangled with the useful foreground features and reduce the inference performance. To help the *inference model* intrinsically distinguishes between the unwanted features and foreground features, in the *training phase*, we repeatedly feed synthetically generated, fake images to the network that have been composed of two components: i) critical parts of the current input image that describe the ground truth labels (i.e., person’s identity), and we would like to have an attention on them, and ii) parts of the other real samples that intuitively are uncorrelated with the current identity (i.e., background and body parts that we would like the network to ignore them). Thereby, compelling the model to look through each region of interest juxtaposed with different undesired areas —of all the images— enables the network to learn where to look at in the image and ignores the parts that are changing arbitrarily and are not correlated with ground truth labels. Consequently, during the test phase, the model not only explores the region of interest but also discards the features of unwanted regions that have been trained for. From a mathematical point of view, let  $I_i, l_i, M_i$  and  $I_j, l_j, M_j$  be two images of the train set that  $I, l$ , and  $M$  represent the image, ground truth labels, and the human binary mask, respectively. If  $ROI_i$  shows the region of interest and  $UR_j$  refers to the unwanted region, then, the goal is to synthesis the artificial sample  $S_{i \rightarrow j}$  with the label  $l_i$ :

$$S_{i \rightarrow j}(x, y) = ROI_i \cup UR_j, \quad (1)$$

where  $ROI_i = I_i(x, y)$  such that  $M_i(x, y) = 1$ ,  $UR_j = I_j(x, y)$  such that  $M_j(x, y) = 0$ , and  $(x, y)$  are the coordinates of the pixels.

Therefore, for an  $N$ -sized dataset, the *maximum* number of generated images is equal to  $N^2 - N$ . However, to avoid losing the expressiveness of the generated samples, we consider several constraints. Hence, a combination of the common data transformations (e.g., flipping, cropping, blurring) can be used along with our method. Obviously, since we uti-

For example, in a hair-color-recognition model, the region of interest is the hair area that can be defined by a binary mask with the same size as the image such that pixels inside the region of interest are set to 1, and all the other pixels are set to 0.

lize the ground truth masks, our technique should be done in the first place before any other augmentation transformation.

### 3.2 Synthetic Image Generation

To ensure that the synthetically generated images have a natural aspect, we impose the following constraints:

**Size and shape constraint.** We avoid combining images with significant differences in their aspect ratios of the ROIs to circumvent the unrealistic stretching of the replaced content or large discontinuities between the body parts in the generated images. To this end, the ratio between the foreground areas defined by masks  $M_j$  and  $M_i$  should be less than the threshold  $T_s$  (we considered  $T_s = 0.8$  in our experiments). Let  $A_i$  be the area of the foreground region (i.e., mask  $M_i$ ):

$$A_i = \sum_{x=0}^W \sum_{y=0}^H M_j(x, y). \quad (2)$$

This constraint translates to  $\min(A_i, A_j) / (\max A_i, A_j < T_s)$ . Moreover, to ensure the shape similarity, we calculate the Intersection over Union metric (IoU) for masks  $M_i$  and  $M_j$ .

By preserving the aspect ratio, the rectangular masks are then cropped and resized to normalize their dimensions. Afterward, if the  $\text{IoU}(M_i, M_j)$  is lower than a threshold  $T_i$ , we consider those images for the merging process.

**Viewpoint constraint.** Body pose is another decisive factor for generating semantically natural images. Thereby, we only combine images with the same viewpoint annotations. For instance, suppose that we are interested in building attention on the human upper-body; therefore, we should avoid generating images composed of anterior upper-body of the  $i$ -th person and posterior lower-body (and background) of the  $j$ -th person. One can apply Alphapose [14] on any pedestrian dataset to estimate the body poses and then, uses [15] to create clusters of poses as the viewpoint label. However, since the RAP dataset annotations include the pose information, we skipped this step in our experiments.

**Smoothness constraint.** Last but not least, the transition between the source image and the replaced content should be as smooth as possible to prevent from inserting any strong edges. As a challenge,  $M_i$  and the body silhouette of the  $j$ -th person do not match perfectly. To overcome this issue, we enlarge the mask  $M_j$  by using the morphological dilation operator with a  $7 \times 7$  kernel:  $M_d = M_j \oplus K_{7 \times 7}$ . Next, to guarantee the continuity between the background and the newly added content, we use the image inpainting technique in [16] to remove the undesired area from the source image, as it has been dictated by the enlarged mask  $M_d$ .

Figure 2 shows some examples generated by our technique, providing attention on the upper-body or full-body region. When enabling the attention on the upper-body region, fake samples are different in the human lower-body and the environment while they resemble each other in the person’s upper-body and identity label. By selecting the full-body as the ROI, the generated images will be composed of similar

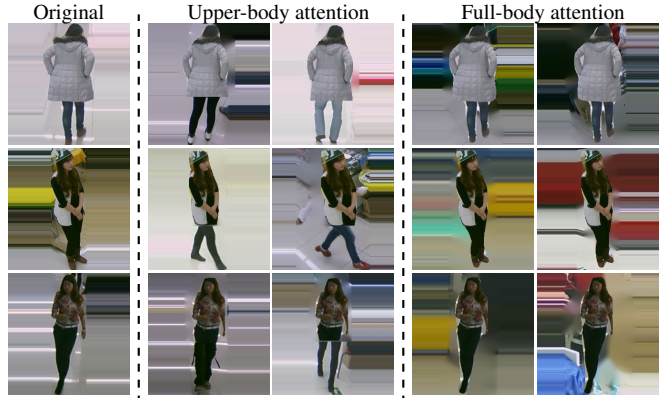


**Fig. 2:** Examples of attentional upper-body (center columns) and full-body (rightmost columns) data augmentation. The leftmost column shows the original images, and the other ones are synthetic samples composed of the original ROI and segments from other individuals. Additional examples are provided at <https://github.com/Ehsan-Yaghoubi/reid-strong-baseline>.

body silhouettes with different surroundings.

## 4 Implementation Details

We based our method on the baseline [17] and selected a similar model architecture, parameter settings, and optimizer. In this baseline<sup>3</sup>, authors resize images on-the-fly into  $128 \times 128$  pixels. Since the RAP images vary in resolution (from  $33 \times 81$  to  $415 \times 583$ ), to avoid any data deformation, we first mapped the images to a squared shape, using *s replication* technique, in which the row or column at the very edge of the original image is replicated to the extra border of the image.

As the RAP dataset does not provide human body segmentation annotations, we first feed the images to MaskRCNN model [18] to obtain human segmentation binary masks; then, as described in subsection 3.2 we generate fake images to enlarge the dataset. We followed the default parameter settings explained on the official project web page<sup>4</sup> and inferred the person masks without modifying the model weights.

To perform the Re-ID process, we followed instructions of [19] and split the dataset to train (1,295 ids), query (1,294 ids), and gallery (1,294 ids) sets including respectively 13, 101, 7, 173, and 13,392 number of samples from 23 different cameras.

## 5 Experiments and Discussion

### 5.1 Datasets

The *Richly Annotated Pedestrian* (RAP) benchmark [19] is the largest well-known pedestrian dataset composing of around 85,000 samples from which 41,585 images have been elected manually for identity annotation. The RAP Re-ID set includes 26,638 images of 2,589 identities and 14,947 samples as distractors that have been collected from 23 cameras in a shopping mall. The provided human bounding boxes have

<sup>3</sup><https://github.com/michuanhaohao/reid-strong-baseline>

<sup>4</sup>[https://github.com/matterport/Mask\\_RCNN](https://github.com/matterport/Mask_RCNN)

different resolutions ranging from  $33 \times 81$  to  $415 \times 583$ . In addition to human attributes, the RAP dataset is annotated for camera angle, body-part position, and occlusions.

## 5.2 Baseline

We selected the work of Luo *et al.* [17] as the baseline method, which has recently advanced the state-of-the-art performance with respect to techniques such as [20],[21] and [22]. Luo *et al.* propose a deep learning-based classification framework, along with a bag of tricks, known to be particularly effective for person Re-ID. They employ the ResNet-50 model as the backbone feature extractor, (initialized with the ImageNet pre-trained parameters) and provide the system implementation upon an open-source library (open-ReID<sup>5</sup>).

## 5.3 Re-ID Results

Following the settings suggested in [17], we re-evaluated the baseline method on the RAP dataset, using the state-of-the-art tricks such as warm-up learning rate [23], random erasing data augmentation [3], label smoothing [24], last stride [25], and BNNeck [17], alongside the conventional data augmentation transformations (i.e., random horizontal flip, random crop, and 10-pixel-padding and original-size-crop).

Table 1 provides the overall performances based on the mean Average Precision (*mAP*) metric and Cumulative Match Characteristic (CMC) for ranks 1, 5, and 10, denoting the possibility of retrieving at least one true positive in the top-1, 5, and 10 ranks. We evaluated both models on two loss functions and observed a slight improvement in the performance of both methods when using the *triplet* loss function over *softmax*. Specifically, the second row in this table suggests that our technique with an attention on the human upper-body improves the results of rank 1 by approximately 5%. However, the higher the rank, the closer the performance values are, such that in rank 10, the improvement is less than 2%. Moreover, *mAP*s improved from 30.4 and 33.5 to 40.2 and 42.4 for *softmax* and *triplet* loss functions, respectively. The third row provides the performance of the proposed method with an attention on the human full-body and indicates that concentration on the full-body yields more useful features for person Re-ID, such that (for the *triplet* loss function) the *mAP* metric improves around 4% more when using the full-body region. Moreover, the retrieving accuracy for ranks 1, 5, and 10 increases to 69.0%, 83.6%, and 88.1%, respectively.

During the training phase, each synthesized sample is generated with a probability between  $[0, 1]$ , with 0 meaning that no changes will be done in the dataset (i.e., we use the original samples) and 1 indicating that all samples will be transformed (augmented). We studied the effectiveness of our method for different probabilities (0.1, 0.3, 0.5, 0.7, 0.9) and depicted the obtained results versus the baseline in Figure 3. Overall, the retrieval accuracy of the proposed technique with an attention on the upper-body surpasses the baseline

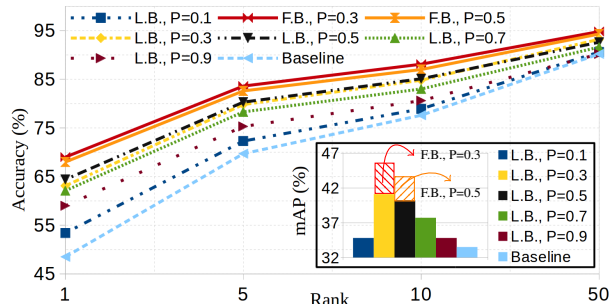


**Fig. 3:** Performance of the proposed augmentation technique for a range of probabilities and ranks versus the baseline [17]. The bar chart compares the *mAP* metric, and the line graph represents the accuracy of the methods for ranks 1, 5, 10, 50. Dark-blue, yellow, black, green, and brown colors show the behavior of our upper-body attention augmentation for probabilities 0.1, 0.3, 0.5, 0.7, and 0.9, and the light-blue color shows the performance of the baseline. Red and orange show the performance of the full-body attention augmentation for probabilities 0.3 and 0.5, respectively. F.B. stands for the full-body, and L.B. is the abbreviation for the lower-body.

**Table 1:** Comparison between the results obtained by the baseline (top row) and our solutions (for developing an attention on the upper body and full body) on the RAP benchmark. *mAP* and Ranks 1, 5, and 10 are given, for the *softmax* and *triplet* loss functions.

	softmax				triplet			
	r=1	r=5	r=10	<i>mAP</i>	r=1	r=5	r=10	<i>mAP</i>
Luo <i>et al.</i> [17]	44.6	66.5	74.6	30.4	48.5	69.7	77.6	33.5
Ours (Upper Body)	62.9	79.8	84.7	40.2	64.8	81.4	85.9	42.4
Ours (Full Body)	<b>65.7</b>	<b>82.2</b>	<b>87.2</b>	<b>45.0</b>	<b>69.0</b>	<b>83.6</b>	<b>88.1</b>	<b>46.3</b>

between 5 to 15 percent for rank 1, with confirming up to 8 percent improvement in *mAP* metric. Developing the attention on the full-body with 0.3 probability improves the *mAP* to %46.3 and the 1<sup>st</sup> rank to %69. By analyzing the trends in Fig. 3, the optimal performance is attained when the augmentation probability lies in the  $[0.3, 0.5]$  interval. This lead us to conclude that such intermediate probabilities of augmentation keep the discriminating information of the original data while also guarantee the transformation of enough data for yielding an effective attention mechanism.

## 6 Conclusions

CNNs are able to autonomously find the critical regions of the input data and discriminate between foreground and background features. However, they demand huge volumes of data, which can be hard to collect and (particularly) annotate for usage in supervised tasks. In this paper, we develop an augmentation technique that empowers the network to improve this autonomous *discovery skill*. During the learning phase, we implicitly provide the network with an attentional mechanism, derived from prior information (i.e., annotations and body masks), that determines the most important regions of the input data. In *test* time, samples are provided without any segmentation mask, which lowers the computational burden with respect to explicit attention mechanisms. As a proof-of-concept, our experiments were carried out in the highly challenging pedestrian re-identification problem, and the results show that our approach contributes for significant improvements in performance over the state-of-the-art.

<sup>5</sup><https://cysu.github.io/open-reid/notes/overview.html>

## 7 References

- [1] Connor Shorten and Taghi M Khoshgoftaar, “A survey on image data augmentation for deep learning,” *J. Big Data*, vol. 6, no. 1, pp. 60, 2019.
- [2] Hiroshi Inoue, “Data augmentation by pairing samples for images classification,” *CoRR*, vol. abs/1801.02929, 2018.
- [3] Zhun Zhong, Liang Zheng, Guoliang Kang, Shaozi Li, and Yi Yang, “Random erasing data augmentation,” in *Proc AAAI Conf*, 2020.
- [4] Ziwei Liu, Ping Luo, Shi Qiu, Xiaogang Wang, and Xiaoou Tang, “Deepfashion: Powering robust clothes recognition and retrieval with rich annotations,” in *Proc IEEE CVPR*, 2016, pp. 1096–1104.
- [5] Misha Denil, Loris Bazzani, Hugo Larochelle, and Nando de Freitas, “Learning where to attend with deep architectures for image tracking,” *Neural Comput.*, vol. 24, no. 8, pp. 2151–2184, 2012.
- [6] Rahul Rama Varior, Mrinal Haloi, and Gang Wang, “Gated siamese convolutional neural network architecture for human re-identification,” in *Proc IEEE ECCV*. Springer, 2016, pp. 791–808.
- [7] Xihui Liu, Haiyu Zhao, Maoqing Tian, Lu Sheng, Jing Shao, Shuai Yi, Junjie Yan, and Xiaogang Wang, “Hydraplus-net: Attentive deep features for pedestrian analysis,” in *Proc IEEE ICCV*, 2017, pp. 350–359.
- [8] Wentong Liao, Michael Ying Yang, Ni Zhan, and Bodo Rosenhahn, “Triplet-based deep similarity learning for person re-identification,” in *Proc IEEE ICCV*, 2017, pp. 385–393.
- [9] Tong Xiao, Hongsheng Li, Wanli Ouyang, and Xiaogang Wang, “Learning deep feature representations with domain guided dropout for person re-identification,” in *Proc IEEE CVPR*, 2016, pp. 1249–1258.
- [10] Niall McLaughlin, Jesus Martinez del Rincon, and Paul Miller, “Recurrent convolutional network for video-based person re-identification,” in *Proc IEEE CVPR*, 2016, pp. 1325–1334.
- [11] Hao Liu, Jiashi Feng, Meibin Qi, Jianguo Jiang, and Shuicheng Yan, “End-to-end comparative attention networks for person re-identification,” *IEEE T IMAGE PROCESS*, vol. 26, no. 7, pp. 3492–3506, 2017.
- [12] Zhedong Zheng, Liang Zheng, and Yi Yang, “Unlabeled samples generated by gan improve the person re-identification baseline in vitro,” in *Proc IEEE ICCV*, 2017, pp. 3754–3762.
- [13] Liqian Ma, Xu Jia, Qianru Sun, Bernt Schiele, Tinne Tuytelaars, and Luc Van Gool, “Pose guided person image generation,” in *Adv Neural Inf Process Syst*, 2017, pp. 406–416.
- [14] Hao-Shu Fang, Shuqin Xie, Yu-Wing Tai, and Cewu Lu, “RMPE: Regional multi-person pose estimation,” in *ICCV*, 2017.
- [15] Laurens van der Maaten and Geoffrey Hinton, “Visualizing data using t-sne,” *Journal of machine learning research*, vol. 9, no. Nov, pp. 2579–2605, 2008.
- [16] Alexandru Telea, “An image inpainting technique based on the fast marching method,” *Journal of graphics tools*, vol. 9, no. 1, pp. 23–34, 2004.
- [17] Hao Luo, Youzhi Gu, Xingyu Liao, Shenqi Lai, and Wei Jiang, “Bag of tricks and a strong baseline for deep person re-identification,” in *Proc IEEE CVPR*, June 2019.
- [18] Kaiming He, Georgia Gkioxari, Piotr Dollár, and Ross Girshick, “Mask r-cnn,” in *Proc IEEE ICCV*, 2017, pp. 2961–2969.
- [19] Dangwei Li, Zhang Zhang, Xiaotang Chen, and Kaiqi Huang, “A richly annotated pedestrian dataset for person retrieval in real surveillance scenarios,” *IEEE T IMAGE PROCESS*, vol. 28, no. 4, pp. 1575–1590, 2018.
- [20] Mahdi M Kalayeh, Emrah Basaran, Muhittin Gökmen, Mustafa E Kamasak, and Mubarak Shah, “Human semantic parsing for person re-identification,” in *Proc IEEE CVPR*, 2018, pp. 1062–1071.
- [21] Zhun Zhong, Liang Zheng, Zhedong Zheng, Shaozi Li, and Yi Yang, “Camstyle: A novel data augmentation method for person re-identification,” *IEEE T IMAGE PROCESS*, vol. 28, no. 3, pp. 1176–1190, 2018.
- [22] Wei Li, Xiatian Zhu, and Shaogang Gong, “Harmonious attention network for person re-identification,” in *Proc IEEE CVPR*, 2018, pp. 2285–2294.
- [23] Xing Fan, Wei Jiang, Hao Luo, and Mengjuan Fei, “Spherereid: Deep hypersphere manifold embedding for person re-identification,” *J VIS COMMUN IMAGE R.*, vol. 60, pp. 51–58, 2019.
- [24] Zhedong Zheng, Liang Zheng, and Yi Yang, “A discriminatively learned cnn embedding for person re-identification,” *ACM TOMM*, vol. 14, no. 1, pp. 13, 2018.
- [25] Yifan Sun, Liang Zheng, Yi Yang, Qi Tian, and Shengjin Wang, “Beyond part models: Person retrieval with refined part pooling (and a strong convolutional baseline),” in *Proc IEEE ECCV*, 2018, pp. 480–496.